Cooperative Binding of ATP and RNA Substrates to the DEAD/H Protein DbpA†

Kevin J. Polach and Olke C. Uhlenbeck*

Department of Chemistry and Biochemistry, UCB 215, University of Colorado, Boulder, Colorado 80309-0215

Received November 16, 2001; Revised Manuscript Received January 16, 2002

ABSTRACT: Unlike most DEAD/H proteins, the purified *Escherichia coli* protein DbpA demonstrates high specificity for its 23S rRNA substrate in vitro. Here we describe several assays designed to characterize the interaction of DbpA with its RNA and ATP substrates. Electrophoretic mobility shift assays reveal a sub-nanomolar binding affinity for a 153 nucleotide RNA substrate (R153) derived from the 23S rRNA. High affinity RNA binding requires both hairpin 92 and helix 90, as substrates lacking these structures bind DbpA with lower affinity. AMPPNP inhibition assays and ATP/ADP binding assays provide binding constants for ATP and ADP to DbpA with and without RNA substrates. These data have been used to describe a minimal thermodynamic scheme for the binding of the RNA and ATP substrates to DbpA, which reveals cooperative binding between larger RNAs and ATP with cooperative energies of ∼1.3 kcal mol^{-1}. This cooperativity is lost upon removal of helix 89 from R153, suggesting this helix is either the preferred target for DbpA's helicase activity or is a necessary structural element for organization of the target site within R153.

DEAD/H proteins are ATP-dependent RNA helicases that serve critical roles in many different cellular processes involving RNA (for reviews, see refs *1*−*6*). Relatively little is known about the mechanism of DEAD/H proteins and what determines their specificity in vivo. Central to an understanding of the helicase mechanism is a thorough analysis of enzyme−substrate interactions and characterization of how those interactions change throughout the ATP hydrolysis cycle. Poor substrate specificity and generally low activities of purified DEAD/H proteins have made detailed mechanistic studies difficult. Although many of these proteins act on specific RNAs in vivo, their specificity appears to require accessory factors that complicate mechanistic analysis. Despite these difficulties, some mechanistic data have been collected for DEAD/H proteins with the most thorough analysis being by Lorsch and Herschlag for the prototypical DEAD/H protein eIF4A (*7*, *8*). Here minimal thermodynamic and kinetic frameworks demonstrate cooperative binding of the ATP and RNA substrates and suggest a cycle of conformational changes within the complex tied to ATP binding and hydrolysis. Kinetic schemes for the vaccinia virus replicative RNA helicase NPH-II (*9*) also suggest cycles of ATP binding, and hydrolysis may drive translocation and helix unwinding, as has been proposed for many DNA helicases, including Rep, DnaB, and UvrD (*10*, *11*).

The *Escherichia coli* DEAD/H protein DbpA[1] and its *Bacillus subtilis* homologue YxiN are very well suited to mechanistic studies since they exhibit high substrate specificity as purified proteins. These proteins contain a 75-amino acid C-terminal domain that defines a subfamily of bacterial DEAD/H proteins (*12*) and is believed to confer RNA specificity. The ATPase activities of both DbpA and YxiN are specifically activated by low concentrations of subfragments of 23S rRNA that include hairpin 92, an essential component of the ribosomal active site (*12*−*15*). Fragments as small as 32 nucleotides stimulate the ATPase activity of DbpA (*16*) and can be adapted to demonstrate helicase activity (*17*).

In this paper, we describe several assays for measuring both ATP and RNA binding to DbpA and put forth a minimal thermodynamic binding scheme describing the interactions. It is evident from this scheme that RNA fragments derived from 23S rRNA contain two discrete elements required for high affinity binding: hairpin 92 and helix 90. We also observe allosteric cooperativity in the binding of the larger RNA substrates and ATP to DbpA in which binding of the ATP increases affinity for the RNA and vice versa. This cooperativity also requires a particular helix from 23S rRNA: helix 89.

MATERIALS AND METHODS

RNA Synthesis. The RNAs R73, R80, and R153 were generated via runoff transcription from linearized plasmids using T7 RNAP (*18*). The R90, R103, R110, and R130 RNAs were transcribed from PCR products that contained T7 promoters and blunt ends that formed run-off templates. The R32 and R19 RNAs were prepared by in vitro transcription using annealed oligonucleotides as transcription tem-

† This work was funded by National Institutes of Health Grant GM60268 to O.C.U. and by a NIH NRSA postdoctoral fellowship (Grant GM20005) to K.J.P.

* Corresponding author. Phone: 303-492-6929. Fax: 303-492-3586. E-mail: Olke.Uhlenbeck@colorado.edu.

[1] Abbreviations: nt − nucleotide; ssRNA − single strand RNA; dsRNA − double strand RNA; TRIS − tris(hydroxymethyl) aminomethane; HEPES − *N*-(2-hydroxyethyl)piperazine-*N*′-(2-ethanesulfonic acid); MOPS − 3-(*N*-morpholino)propanesulfonic acid; TBE − 90 mM Tris-borate (pH 8.0), 2 mM ethylenediaminetetraacetate; DTT − dithiothreitol; BSA − bovine serum albumin; DEAE − diethylaminoethyl; eIF4A − eukaryotic initiation factor 4A.; NPHII − nucleotide triphosphate phosphohydrolase (vaccinia virus RNA helicase); DbpA − dead box protein A.

10.1021/bi012062n CCC: $22.00
Published on Web 02/16/2002

plates. Transcription reactions were performed on a 1 to 5 mL scale as described (*18*). Pyrophosphate was removed by centrifugation, and products were extracted once with phenol/chloroform, three times with chloroform, and subsequently precipitated with ethanol. Precipitated RNAs were then purified from remaining NTPs by sequential gel filtration and DEAE sepharose columns. Product elution was monitored via absorbance at 260 nm, and RNA-containing fractions were pooled and ethanol precipitated. Precipitated RNAs were washed 3 times with 70% ethanol and resuspended in 10 mM HEPES (pH 7.5) and stored at −20 °C.

DbpA Protein Preparation and Purification. DbpA was overexpressed in *E. coli* from a plasmid containing a T7 promoter and purified as described previously (*14*). DbpA stocks were concentrated into storage buffer consisting of 20 mM MOPS (pH 6.8), 50 mM NaCl, 1 mM DTT, and 50% glycerol. The concentration of the stock was calculated from the absorbance signal at 280 nm using an extinction coefficient calculated from the amino acid composition (ϵ^{280} = 27 680 M^{-1} cm^{-1}) in 6.0 M guanidine hydrochloride.

Electrophoretic Mobility Shift Assays. RNA substrates (400 ng) were 5′-^{32}P-labeled with polynucleotide kinase and purified on 10% denaturing polyacrylamide gels. Product bands were cut out, and labeled RNAs were soaked out of the gel slices overnight in 750 μL of 10 mM HEPES (pH 7.5). Supernatants were removed from gel pieces, and labeled RNAs were precipitated with ethanol.

Binding reactions were carried out in 10 mM HEPES (pH 7.5), 50 mM KCl, 5 mM $MgCl_2$, 100 μM DTT, 100 μg/mL BSA, and 5% glycerol (binding buffer 1). Ten microliter reactions were prepared with 10 pM labeled RNA, 70 μM polyA competitor (in bases), and increasing amounts of DbpA protein. Samples were equilibrated for 30 min at room temperature and loaded to 5% native acrylamide gels (29:1 acrylamide to bis) running at 20 V/cm in 1/3× TBE at room temperature. Gels were run for ∼1 h, dried, and exposed to a phosphorimager screen. The fraction of bound material was calculated by quantifying the number of counts in the shifted vs unshifted bands after subtracting a background from areas below the bands. The fraction of bound material was then plotted against protein concentration and fit to sigmoid binding curves: $Y = [X/(M1 + X)]M2$, where M1 is the dissociation constant (K_d) and M2 is the upper plateau of the binding curve. Results from 5 to 8 separate binding reactions were compiled and averaged, with typical errors of < 15% among duplicate binding sets.

ATP/ADP Binding Assays. ATP/ADP binding by DbpA was examined via an equilibrium filtration experiment. Labeled nucleotides [2.5 nM γ-^{32}P ATP (6000 Ci/mmol), 17 nM γ-^{35}S ATP (600 Ci/mmol), 0.37 μM ^{3}H AMPPNP (27 Ci/mmol), or 0.4 μM ^{3}H ADP (25 Ci/mmol)] were equilibrated for 30 min with 10−40 μM DbpA in 100 μL reactions containing binding buffer 1. Binding assays performed in the presence of RNA contained equimolar amounts of RNA and DbpA protein. Binding reactions were then loaded to a centrifugal filter device (10-kDa cutoff), and 5 μL was spun through the filter. Disturbances to the equilibrium were minimal, since only 5% of the total binding reaction was passed through the filter. One microliter aliquots were collected (in triplicate) with microcapillary pipets from above and below the filter, added to scintillation cocktail, and counted in a Beckman LS 3801 scintillation counter.

Assuming a simple nucleotide binding site and fully active protein, the ratio (R) of counts above the filter ([bound nucleotide] + [free nucleotide]) to counts below the filter ([free nucleotide]) is related to the dissociation constant (K_d) by the following: $(R - 1) = (1/K_d)$[DbpA]. When $R - 1$ is plotted as a function of the DbpA concentration, the resulting linear relation has a slope equal to $1/K_d$. For each nucleotide, at least four different DbpA concentrations were used to confirm the value of K_d (Figure 4).

AMPPNP Inhibition Assays. ATPase activity was monitored via a coupled spectroscopic assay described previously (*14*). Reactions were prepared containing 10 mM HEPES (pH 7.5), 50 mM KCl, 5 mM $MgCl_2$, 100 μM DTT, 5% glycerol, 1 mM phosphoenolpyruvate, 150 units of pyruvate kinase, 280 μM NADH, 210 units of lactic dehydrogenase, 2 nM DbpA, and saturating amounts of RNA (50 nM R153mer and 100 nM R80mer). ATP hydrolysis (ADP generation) is coupled to NADH oxidation and detected by the corresponding change in absorbance at 338 nm, which are converted to picomoles of ATP hydrolyzed per picomole of DbpA per minute. Titrations of ATP·Mg were carried out in the presence of increasing amounts of AMPPNP·Mg, and ATP hydrolysis rates were measured for each set of conditions. Double reciprocal plots were prepared for each experiment, and least-squares fits to linear equations yielded slopes and y intercepts ($1/K_M$(app) values) for each inhibitor concentration. Replots of slopes and K_M(app) values vs the AMPPNP concentration yielded the inhibition constants for AMPPNP for each of the protein−RNA complexes.

RESULTS

An Effective RNA Binding Assay. Previous work on the ATPase activity of DbpA indicate that the apparent binding affinities for RNA and ATP substrates depend on the identity of the RNA molecule used (*16*). However, binding affinities deduced from the ATPase assay potentially contain components of the binding steps, the chemical step, and other kinetically significant steps in the overall hydrolysis reaction under multiple turnover conditions. It was therefore desirable to develop direct binding assays to obtain elementary binding constants for each substrate in the presence and absence of the other.

While the very tight binding of RNA to DbpA complicates the use of fluorescence assays, filter binding is an attractive option due to its high sensitivity, minimal disturbance to the equilibrium, and adaptability to high throughput (*19*, *20*). Although filter retention of RNA by DbpA can be observed, the protein does not denature upon filter binding and thus can trap free RNA as it passes through the filter (Kossen and Uhlenbeck, unpublished results). As a result, the amount of RNA bound to the filter does not correctly report on the fraction of complex in solution prior to filtration thereby making the assay unusable. An electrophoretic mobility shift assay established for DbpA (R. Story, personal communication; *21*, *22*) is potentially well suited to measuring the DbpA−RNA interaction in a quantitative manner. At neutral pH, DbpA is slightly basic and DbpA−RNA complexes are acidic, so free protein should rapidly separate from free RNA and complex as soon as an electric field is applied. The free RNA and complex will subsequently enter the gel and be separated due to differences in size and net charge.

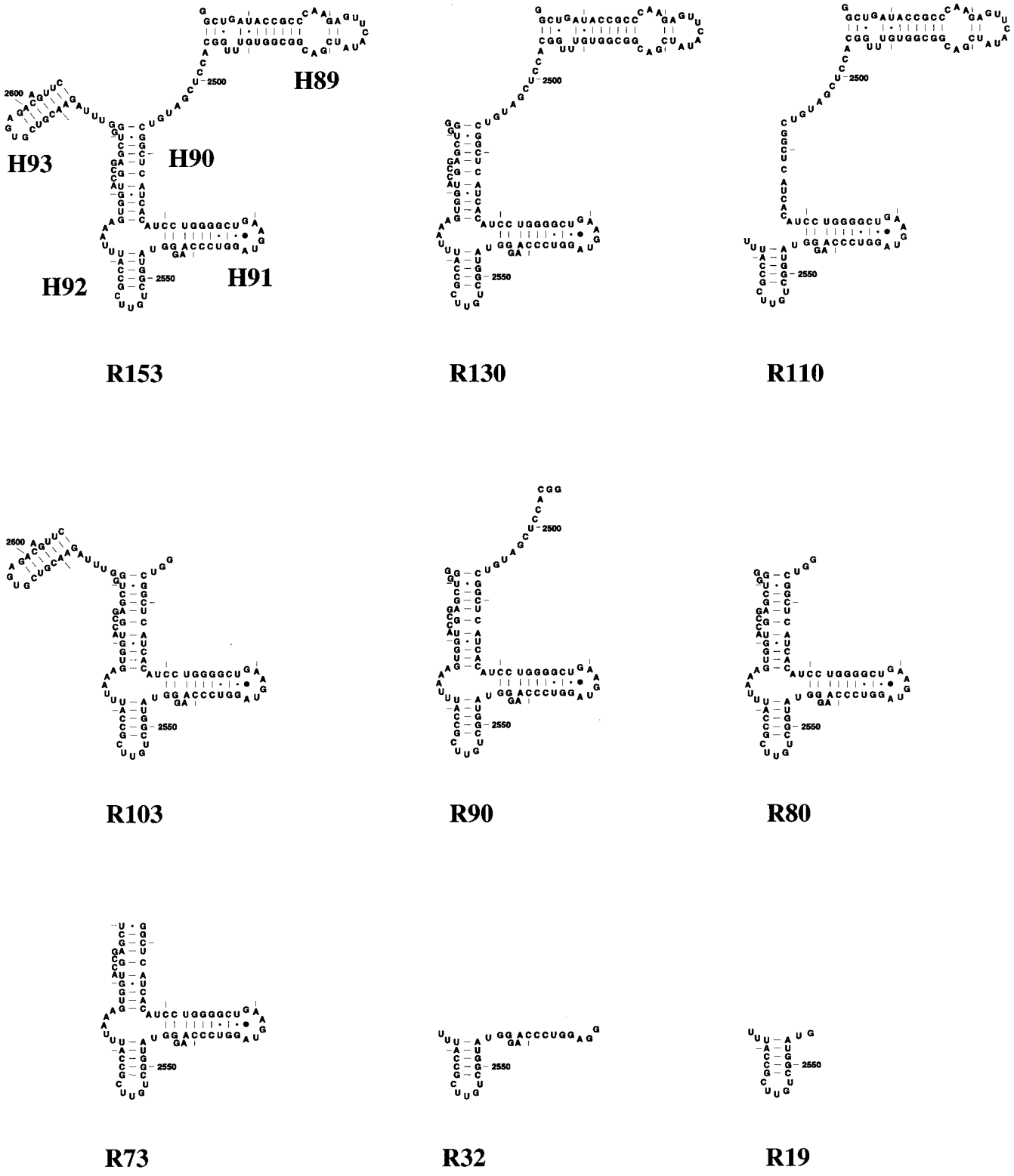

FIGURE 1: Derivatives of the 23S rRNA used in these studies. Fragment structures drawn based on secondary structures present in 23S rRNA.

The interaction of DbpA with RNA was first examined using R153 (Figure 1), a 153-nucleotide fragment of 23S rRNA that contains five helices and fully stimulates the ATPase activity (*13*, *14*). A subsaturating concentration of R153 (5′-^{32}P-labeled to a high specific activity, [R153] $\ll K_d$) was mixed with a wide range of DbpA concentrations and subjected to electrophoresis on 5% native polyacrylamide gels. As shown in Figure 2A, a defined protein−RNA complex of lower mobility than the free probe is observed early in the titration, while several bands of decreasing mobility are seen as the DbpA concentration exceeds 10 nM. These data indicate the formation of one high affinity complex as well as several lower affinity complexes that probably contain several protein molecules. As shown in Figure 2B, the low affinity binding component can be suppressed by addition of polyA competitor, greatly sim-

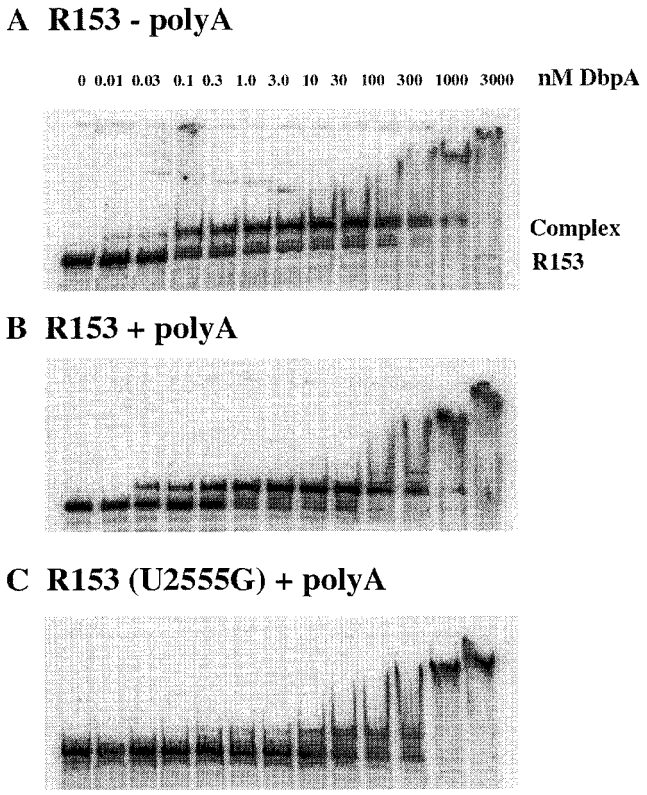

FIGURE 2: Electrophoretic mobility shift assay. (A) The indicated concentrations of DbpA are mixed with 10 pM ^{32}P-labeled R153 in 10 mM HEPES (pH 7.5), 50 mM KCl, 5 mM $MgCl_2$, 100 μM DTT, 100 μg/mL BSA, and 5% glycerol and applied to a 5% native acrylamide gel. (B) The same experiment as A with 70 μM polyA competitor (in bases). (C) The same experiment as B with U2555G mutation in R153.

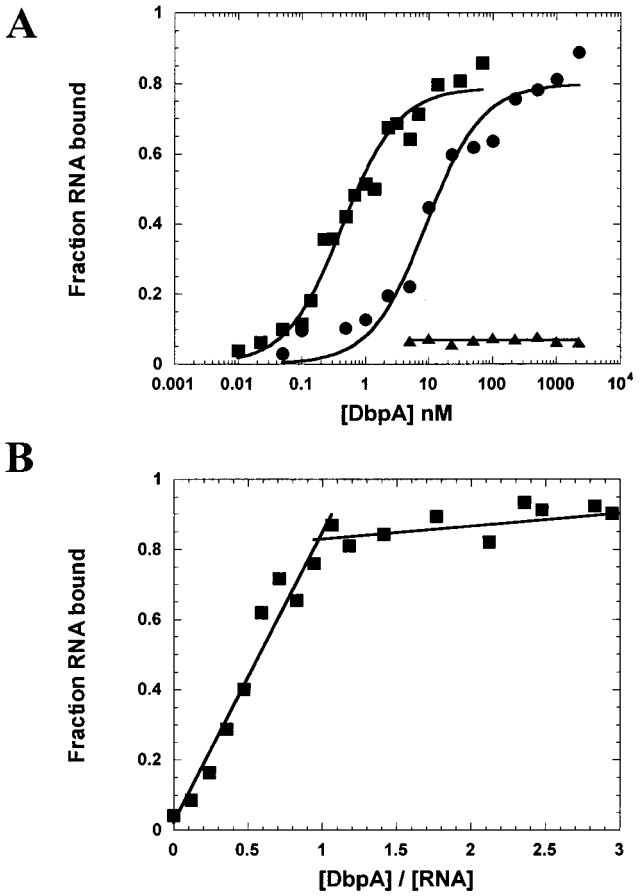

FIGURE 3: Binding affinities and stoichiometry. (A) The fraction of RNA in complex determined in gel shift assays plotted as a function of protein concentration for R153 (squares), R32 (circles), and R19 (triangles). Curves are best fits to a simple binding equilibria with K_d = 0.44 nM and saturation = 0.79 for R153 and K_d = 9.20 nM and saturation = 0.80 for R32. (B) Stoichiometry of R153 binding to DbpA. 58 nM R153 was mixed with varying concentrations of DbpA. The linear increase in fraction RNA bound saturates at 55 nM DbpA.

plifying the analysis of the high affinity binding interaction. A similar titration in which the labeled RNA contains a U2555G mutation in hairpin 92 shows formation of the high affinity complex at significantly greater concentrations of DbpA, although formation of the low affinity complexes is unaffected (Figure 2C). Since hairpin 92 has previously been shown to be a critical element for the stimulation of the ATPase of DbpA (*16*), it appears that the high affinity complex reflects sequence specific binding of RNA by DbpA, while the low affinity complexes are not sequence specific. These low affinity complexes probably reflect nonspecific ionic interactions between RNA and the very basic C-terminal domain of DbpA and are not likely to be relevant to the function of DbpA.

Quantitative analysis of the DbpA titration reveals data that can be fit accurately to a simple, noncooperative binding equation with an apparent K_d of 0.44 nM (Figure 3A). Titrations carried out with variable equilibration times demonstrate the complex is fully formed in less than 3 min (data not shown). The binding curve does not change significantly as a function of the electrophoresis time, the distance the complex travels on the gel, or the percentage of acrylamide used in the gel (data not shown). There is little smearing of counts between the free and bound probe (Figure 2B), indicating that breakdown of the complex during the 1 h of electrophoresis is negligible. While little dissociation of the RNA−protein complex is observed in the gel, preliminary kinetic experiments suggest that in solution the complex is in rapid equilibrium with free RNA. Association rate measurements done in manual mixing experiments reveal a fast rate, although it is too fast to be accurately measured in this system (data not shown). Measurements of the dissociation rate by dilution of equilibrated complexes or by addition of high concentrations of nonlabeled R153 competitor suggest a dissociation rate of >3 min^{-1}. The unexpected stability of dynamic complexes in gel systems has been observed in similar studies of protein−DNA interactions (*23*−*26*) and has been described by several theoretical studies as the cage effect (*27*−*29*). An excellent example is trp repressor binding to an operator DNA that displays a gel mobility shift with a K_d = 0.5 nM and rapid on and off rates, similar to DbpA binding to R153. Although simulations of this interaction require a physical model including a stabilizing effect from the gel, binding constants obtained from the gel are accurate (*24*, *28*).

To relate the apparent K_d in Figure 3A to the actual K_d value, the stoichiometry of the complex and the fraction of active RNA and protein must be known. Since >80% of the RNA appears in the shifted complex band of the gel under a variety of conditions, it is clear that virtually all of the RNA is competent for binding. To determine stoichiometry, a saturating concentration of R153 ([R153] $\gg K_d$) is mixed with increasing amounts of DbpA until saturation is achieved.

Both the slope and the plateau of such a titration reveal a 1:1 stoichiometry of DbpA to RNA in the shifted complex. These data agree with previous measurements of stoichiometry using the ATPase assay (*14*). Together, these assays demonstrate that the RNA stocks are fully competent for binding and the DbpA stocks are fully active. Therefore, measurements of K_d at subsaturating R153 ([RNA] $\ll K_d$) reveal the true K_d value.

The gel shift assay was used with subsaturating RNA concentrations to obtain K_d values for a series of fragments of R153, many of which had been assayed previously for ATPase activity (Figure 1, *14*). In all cases, except R19, simple noncooperative binding curves were obtained where ~80% of the RNA bound at saturation (Figure 3A). Affinities for all fragments are listed in Table 2 and compared to K_{app}(RNA) values previously determined by ATPase assays carried out under the same buffer conditions at 37 °C. All RNA fragments, except R110 and *R*32, bound with K_d values of 0.3 to 0.5 nM. R110 and R32, which both lack an intact helix 90, bound about 20-fold more weakly.

ATP/ADP Binding. Since little change in the intrinsic fluorescence of DbpA was observed upon ATP binding (Tsu and Uhlenbeck, unpublished results), binding constants of several radiolabeled nucleotides to DbpA were determined using an equilibrium filtration assay. Labeled nucleotides were equilibrated for 30 min with DbpA protein, and free probe was separated from bound probe on centrifugal filter devices (10-kDa cutoff). Disturbances to the equilibrium are minimal, since only 5% of the total binding reaction was passed through the filter. Assuming a simple nucleotide binding site and fully active protein, the ratio (*R*) of counts above the filter ([bound nucleotide] + [free nucleotide]) to counts below the filter ([free nucleotide]) is related to the dissociation constant K_d by the following: $(R - 1) = (1/K_d)$[DbpA] (*30*).

In the absence of an RNA substrate, ATP hydrolysis is very slow ($k_{cat} = 0.25$ min^{-1}) allowing for direct binding assays with labeled ATP with minimal hydrolysis of the labeled probe. DbpA shows little discrimination in binding ADP or ATP ($K_d = 44$ and 36 μM, respectively), suggesting that any preference for site occupancy by ATP in the cell is driven by concentration differences (Figure 4 and Table 1). Interestingly, DbpA binding to AMPPNP is greatly reduced ($K_d > 1300$ μM, a lower limit deduced from the slight slope present in the data, taking into account the associated errors from multiple experiments) indicating that although the absence of the γ-phosphate is not detrimental to binding, an incorrect geometry at that position is not well tolerated. Structural analysis of myosin complexed with Mg·AMPPNP, Mg·ATPγS, and Mg·ADP reveal changes in the hydrogen bonding pattern within the ATP binding pocket due to the presence of the bridging nitrogen in AMPPNP (*31*) that could explain the lowered affinity.

Allosteric Cooperativity in the Binding of Nucleotides and RNA. Since eIF4A, Ded1p, and several DNA helicases show cooperative binding of nucleotide and RNA (*8*, *32*−*36*), several experiments were designed to investigate this phenomenon with DbpA. In the first experiment, the ATPase activity of DbpA was measured as a function of R153 concentration in the presence of either subsaturating or saturating ATP concentrations. Apparent binding constants derived from these assays report on RNA binding to free DbpA and the DbpA−ATP complex, respectively. As shown in Figure 5, the apparent binding affinity of R153 to DbpA in the presence of ATP (K_{app}(R153) = 2.8 nM) is considerably tighter than to DbpA alone (K_{app}(R153) = 86 nM).

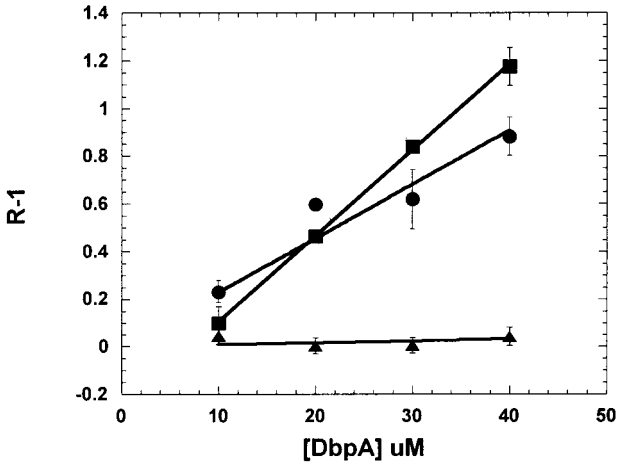

FIGURE 4: Nucleotide affinities determined from filtration binding assays. 25 nM α-^{32}P ATP or 25 nM ^{3}H AMPPNP is mixed with varying concentrations of DbpA in 10 mM HEPES (pH 7.5), 50 mM KCl, 5 mM $MgCl_2$, 100 μM DTT, 100 μg/mL BSA, and 5% glycerol and equilibrated for 30 min prior to filtration. Relations between $R - 1$ (fraction bound/1 − fraction bound) and DbpA concentration are plotted for ATP (squares), ADP (circles), and AMPPNP (triangles), lines are best fits with $K_d = 36$ μM for ATP, $K_d = 44$ μM for ADP, and $K_d > 1.3$ mM for AMPPNP.

Table 1: Nucleotide Binding Affinities

protein or complex	K_d(ADP) (μM)	K_d(ATP) (μM)	K_d(AMPPNP) (μM)	K_M(ATP)[a] (μM)	cooperativity present
DbpA	44	36	>1300		
DbpA−R153	39		21	120	+
DbpA−R80	60		>1300	510	

[a] Data taken from ref *16*.

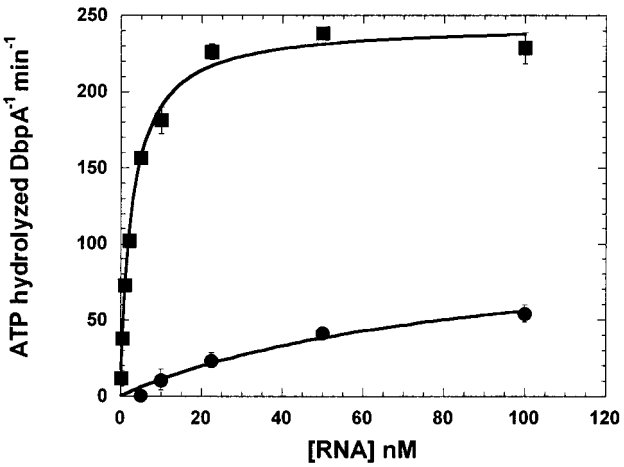

FIGURE 5: Cooperative binding in ATPase assays. ATPase activity is monitored as a function of RNA concentration and ATP hydrolyzed DbpA^{-1} min^{-1} is plotted as a function of R153 concentration under conditions of saturating (squares) and subsaturating (circles) amounts of ATP. Lines are best fits to the Michaelis-Menton equation with K_{app}(R153+ATP) = 2.8 nM and $k_{max} = 240$ ATP hydrolyzed DbpA^{-1} min^{-1} in the presence of saturating ATP and K_{app}(R153) = 86 nM and $k_{max} = 100$ ATP hydrolyzed DbpA^{-1} min^{-1} in the presence of subsaturating ATP.

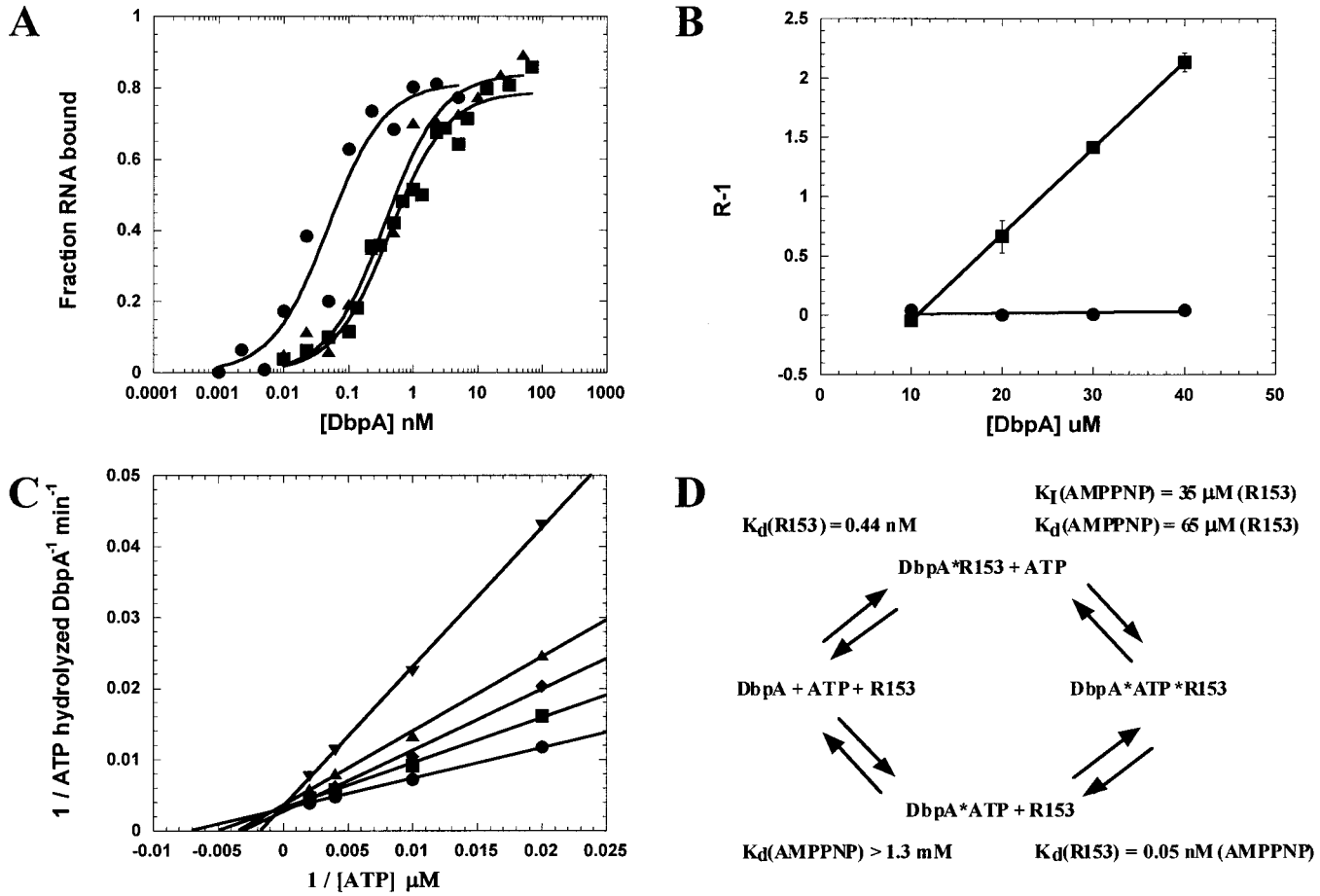

FIGURE 6: Cooperative binding between ATP and RNA substrates. (A) DbpA titrations of R153 (squares), R153 + AMPPNP (circles), or R153 + ADP (triangles). Curves are best fits to a simple binding equilibria with $K_d = 0.44$ nM and saturation = 0.79 for R153, $K_d = 0.05$ nM and saturation = 0.81 for R153 + AMPPNP, and $K_d = 0.37$ nM and saturation = 0.84 for R153 + ADP. (B) Microcon filter assays carried out in the presence and absence of R153. Relations between $R - 1$ and DbpA concentration are plotted, lines are best fits with $K_d > 1.3$ mM for AMPPNP (circles) and $K_d = 21$ μM for AMPPNP + R153 (squares). (C) A double reciprocal plot for the ATPase activity of DbpA in the presence of saturating levels of R153mer and 0 (circles), 10 (squares), 25 (diamonds), 50 (triangles), and 100 (inverted triangles) μM AMPPNP inhibitor. (D) A minimal thermodynamic scheme for R153 and AMPPNP binding to DbpA.

Under the conditions chosen for the assay, the free energy of binding the RNA increases by 2.2 kcal mol^{-1} in the presence of ATP, thereby defining a cooperative binding free energy, ΔG_{coop}.

In an attempt to observe the cooperativity in a direct binding assay, the ability of saturating amounts of ATP to affect RNA binding was investigated using the gel shift assay. Neither the presence of 2 mM ATP nor the slowly hydrolyzable ATPγS affected the binding affinity of R153 at either 25 or 4 °C, even when ATP was added to the gel and recirculated in the electrophoresis buffers (data not shown). However, when the non-hydrolyzable ATP analogue AMPPNP was added to the binding reactions and applied to the gel, a 10-fold higher affinity of DbpA to R153 was observed, indicating cooperative binding of the two substrates (Figure 6A). In this assay, the 10-fold change in affinity corresponds to $\Delta G_{coop} = 1.3$ kcal mol^{-1} in the presence of AMPPNP, slightly less than the value obtained from the enzymatic assay and possibly reflecting differences in the structures of ATP and AMPPNP. Binding assays treated with ADP prior to loading on the gels showed no increase in the binding affinities (Table 1). Thus, cooperative binding is dependent on the presence of a γ-phosphate in the nucleotide.

The enhanced binding of DbpA to R153 in the presence of saturating AMPPNP predicts enhanced binding of AMPPNP in the presence of saturating R153. The affinity of AMPPNP to the DbpA−R153 complex determined by the microcon filtration assay gave a K_d(AMPPNP) = 21 μM, which is at least 60-fold tighter than AMPPNP binding to DbpA without RNA (Figure 6b and Table 1). As expected, little difference is observed in the value of K_d for ADP to DbpA in the presence or absence of R153. A second means for obtaining the binding affinity of AMPPNP involves determining its K_I value in the RNA dependent ATPase activity assay. In this experiment, the rate of ATP hydrolysis by DbpA with saturating R153 is determined with a given concentration of AMPPNP and a series of ATP concentrations to generate an inhibition plot (Figure 6C). The experiment is repeated at several AMPPNP concentrations and a K_I value is deduced. The observed K_I value of 35 μM agrees well with the affinity measured for AMPPNP in the presence of R153 ($K_d = 21$ μM) determined by the direct binding assay.

A summary of the binding properties of DbpA to R153 with and without AMPPNP is presented in Figure 6D as a thermodynamic scheme. It is clear that the binding of R153 to DbpA is cooperative with AMPPNP, and the cooperative free energy is approximately the same when measured by

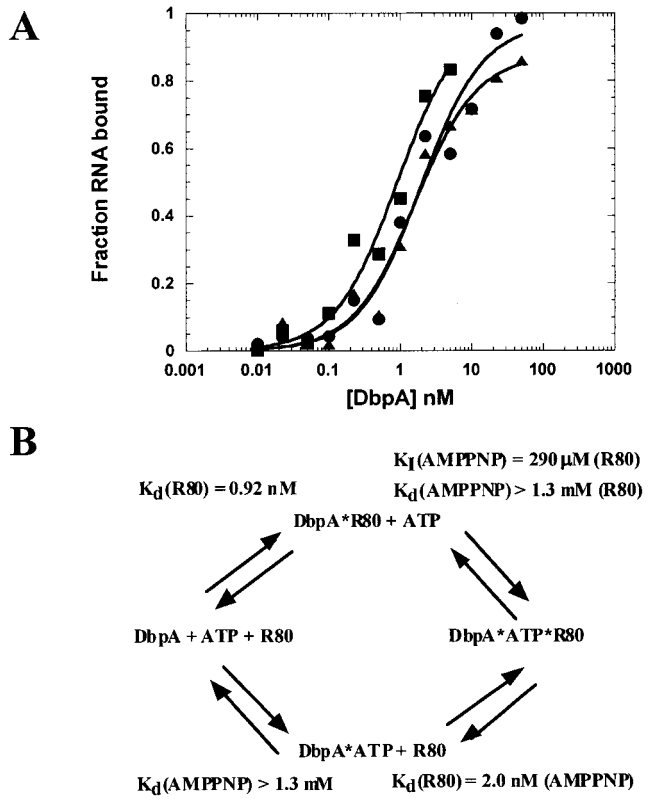

FIGURE 7: Cooperative binding between ATP and RNA substrates depends on RNA identity. (A) DbpA titrations of R80 (squares), R80 + AMPPNP (circles), or R80 + ADP (triangles). Curves are best fits to a simple binding equilibria with K_d = 0.92 nM and saturation = 0.99 for R80, K_d = 1.97 nM and saturation = 0.97 for R80 + AMPPNP, and K_d = 1.64 nM and saturation = 0.88 for R80 + ADP. (B) A minimal thermodynamic scheme for R80 and AMPPNP binding to DbpA.

either RNA or nucleotide binding. This cooperativity is likely to be important to the functional cycle of DbpA, since it is not observed with ADP and thus changes as a function of the ATP hydrolysis cycle.

Cooperative Binding Requires a Specific RNA Element. Previous experiments have shown that the value of K_M(ATP) or K_I(AMPPNP) depends on the identity of the RNA used (*16*). To test whether this phenomenon was related to cooperative binding of ATP and RNA, another fragment of 23S rRNA, R80, was used to perform the same set of experiments performed with R153 in the previous section. Quite strikingly, experiments with R80 carried out in the presence or absence of AMPPNP show no indication of cooperative binding (Figure 7A). Complimentary experiments measuring direct binding of AMPPNP to the DbpA−R80 complex confirm the absence of cooperativity (Table 1).

To understand which sequence elements present in R153 are responsible for cooperative binding, K_d(RNA) was measured for all the RNA fragments shown in Figure 1 in the presence and absence of AMPPNP. Inhibition constants for AMPPNP were also measured at saturating concentrations of each RNA. The results of these experiments are summarized in Table 2. Cooperativity can be assessed by comparing K_d(RNA) with and without AMPPNP and by comparing the measured values of K_I(AMPPNP) for each RNA. Both of these experiments reveal helix 89 as the RNA element required for cooperative binding, as all RNA fragments containing this helix show cooperativity. Even R110, a fragment that binds with a 20-fold lower affinity than R153, shows the same amount of cooperative free energy.

Table 2: RNA Affinities and Requirements for Cooperative Binding

RNA	K_d(RNA) (nM)	K_d(RNA) + AMPPNP (nM)	K_{app}(RNA) (nM)[a]	K_I (AMPPNP) (μM)	coop energy (δ) (kcal mol^{-1})
23S+16S rRNA			24	66	+[b]
R153	0.44	0.05	11	35	1.3
R130	0.35	0.03		70	1.5
R110	8.1	1.0		64	1.2
R103	0.50	0.83		330	*c*
R90	0.43	0.51		260	*c*
R80	0.97	2.0	41	290	*c*
R73	0.30	0.78	360	390	*c*
*R*32	9.2	7.6	700	350	*c*

[a] Data taken from ref *16*. [b] Calculation of cooperative energy not possible since 23S rRNA is too large for the band shift assay, but cooperativity is evident from comparison of K_I measurements. [c] In these cases, calculated cooperative energies are not significant relative to the associated errors in the affinity measurements.

DISCUSSION

RNA Binding and Specificity. DbpA binds to R153 with K_d = 0.44 nM and a total binding energy of 12.8 kcal mol^{-1} in the presence of excess polyA competitor and in the absence of any nucleotide. R153 contains five helices that could contribute to the binding energy and our binding studies allow us to assign relative importance of each helix to the protein−RNA interaction. Hairpin 92 and helix 90 each make similar contributions to the total binding energy, as deletion of helix 90 or mutations within hairpin 92 result in similar decreases in affinity. Removal of helix 93 or disruption of helix 91 has no affect on affinity, suggesting these elements do not contribute to the binding energy and are not required RNA structural elements for DbpA binding. Helix 89 is required for AMPPNP dependent cooperative binding that lowers K_d to 0.05 nM and increases the total binding energy of the system to 14.1 kcal mol^{-1}.

Previous studies of DbpA binding to 23S rRNA fragments establish that the RNA substrate selectivity exhibited by DbpA's ATPase activity occurs at the level of RNA binding (*21*). Whereas R73 formed a specific complex with DbpA, a nonspecific RNA (nt 2418−2475) from 5′ of R73 failed to bind. Although this study was performed in a similar buffer and also utilized the gel shift assay, the binding affinity of DbpA to R73 showed a K_d value of 150 nM, significantly higher than our measured K_d value of 0.3 nM. This discrepancy can be attributed to the concentration of labeled probe in the previous assay, which at 20 nM greatly exceeds our observed binding constant. Under these conditions, lower levels of binding are observed at lower protein concentrations simply because DbpA is not in excess of the probe; thus, the observed K_d overestimates the true K_d. In our experiments, very high specific activity probe was used so that protein was in excess under all conditions.

Nucleic acid binding proteins often show both specific and nonspecific binding properties. A study of DbpA binding to

a nonspecific helicase substrate reveals a $K_d = 300$ nM (*22*) in excellent agreement with our measurements of nonspecific binding to 23S rRNA fragments at high protein concentration. DbpA clearly displays specific and nonspecific binding modes, each of which is capable of supporting ATP-dependent helicase activity (*17*, *22*). At this time, it is not clear that the nonspecific activity is relevant to the function of the enzyme in vivo, given that both the binding and activity of DbpA show such selectivity for the peptidyl transferase center of 23S rRNA.

Direct Binding Constants and Apparent Binding Constants. The elementary binding constants of the RNA and nucleotide substrates, each in the presence of saturating concentrations of the other, can be compared with the K_M(ATP) and K_{app}(RNA) values determined by the RNA dependent ATPase and RNA helicase assays performed under similar conditions. However, it is important to realize that the latter are complex binding constants that represent multiple steps in the reaction pathway and are only expected to equal the elementary binding constants under special circumstances. In the case of the nucleotide substrate, the dissociation constant of AMPPNP determined by the direct binding assay ($K_d = 21$ μM) or by the inhibition assay ($K_I = 35$ μM) closely approximate K_M(ATP) determined by the RNA dependent ATPase assay ($K_M = 120$ μM). Considering that AMPPNP is not the correct substrate, the agreement is excellent, suggesting that k_{-1} is fast compared to the very rapid k_{cat} observed in the ATPase assay ($k_{cat} = 250$ min^{-1}, 25 °C). With a diffusion controlled association rate of 3×10^{10} M^{-1} min^{-1} and a dissociation constant of 21 μM, the calculated dissociation rate of 6×10^5 min^{-1} certainly supports this hypothesis.

In the case of the RNA substrates, the apparent binding constant for a bimolecular version of R32 obtained from a single turnover helicase assay ($K_{app} = 20$ nM) is in excellent agreement with our observed K_d value for R32 of 7.6 nM. This agreement can be understood from current estimates of the rates, since the helicase assay shows a $k_{cat} = 0.2$ min^{-1} and k_{-1} for the RNA is greater than 3 min^{-1}. However, apparent binding constants for RNA substrates measured though multiple turnover ATPase assays are significantly higher than direct binding constants from gel shift assays. For R32, the apparent binding constant ($K_{app} = 700$ nM) is 92-fold higher than the direct binding constant in the presence of AMPPNP ($K_d = 7.6$ nM) and 35-fold greater than the apparent binding constant from the single turnover helicase assay ($K_{app} = 20$ nM). Similar differences exist for all RNA substrates and imply that these apparent binding constants include contributions from either the chemical step or other kinetically relevant steps in the mechanism. At this point, it is difficult to discern the source of this phenomenon since measurement of RNA binding through ATPase activity is indirect. This observation could have significant ramifications for the mechanism of DbpA activity, and further experiments to characterize the phenomenon are underway.

Allosteric Cooperativity in the Binding of ATP and RNA Substrates. Cooperative binding between nucleic acid and ATP substrates has been observed for many DNA helicases (*33*−*35*) and the DEAD/H proteins eIF4A and Ded1p (*7*, *32*). This cooperativity is often dependent on the presence of the γ-phosphate, making binding events in the nucleic acid binding pocket responsive to the ATP hydrolysis cycle. This γ-phosphate sensor has been observed in many other NTPases including well characterized molecular motors such as kinesin (*37*, *38*) and myosin (*39*−*41*), and also in many G-proteins (*42*−*44*). Cycles of ATP binding and hydrolysis have been used to describe mechanisms by which chemical energy from ATP hydrolysis may be converted to mechanical work (for reviews, see refs *11*, *45*−*49*). Cooperative binding of RNA and ATP substrates is indicative of nucleotide-dependent conformational changes in the RNA−protein complex which couple ATP hydrolysis and unwinding by guiding the reaction along the properly coupled pathway.

Cooperative binding of RNA and ATP substrates to DbpA was first evident in measurements of apparent binding constants in ATPase activity assays (*16*). This cooperativity can also be observed by comparing K_{app}(RNA) from ATPase assays done with saturating and subsaturating amounts of ATP (Figure 5). Attempts to measure cooperativity in direct RNA binding assays including either ATP or the slowly hydrolyzable analogue ATP-γS failed to reveal cooperative binding. Since both ATP and ATP-γS are rapidly hydrolyzed by the DbpA−R153 complex, it is likely that turnover is too rapid to observe cooperative binding during the slow time scale of this equilibrium assay. The complexes resolved in these experiments result from a cycling, asynchronous system and most likely represent a heterogeneous mix of intermediates along the hydrolysis pathway, only some of which would be expected to display cooperativity. Consistent with this hypothesis, addition of the non-hydrolyzable analogue, AMPPNP, revealed cooperative binding similar to that observed in the ATPase assays.

In the presence of AMPPNP, DbpA binds R153 with $K_d = 0.05$ nM bringing the total binding energy to 14.0 kcal mol^{-1}. Thus, the binding energy gained through cooperativity ($\Delta G_{coop} = 1.3$ kcal mol^{-1}) is of the same order as the energetic contribution from the two specific binding interactions. Even R110, which lacks an intact helix 90 and shows a substantially decreased overall affinity, displays fully cooperative binding with AMPPNP ($\Delta G_{coop} = 1.2$ kcal mol^{-1}). The independence of high affinity binding and cooperative binding with AMPPNP may indicate the presence of two autonomous RNA binding surfaces on the DbpA protein.

An RNA Element Required for Cooperativity. The novel aspect of DbpA's cooperativity is the requirement not only for the γ-phosphate of the ATP, but also for helix 89 in the RNA substrate. This may suggest direct contacts between DbpA and helix 89 and since the cooperativity responds to the ATP hydrolysis cycle, these contacts may occur through DbpA's helicase site and be required for formation of an optimal initiation complex. Many DEAD/H proteins require helicase substrates with 5′ or 3′ single-stranded regions to form entry complexes and be active (*32*, *50*−*53*) and helix 89 is preceded at the 3′ end by a large single-stranded region in each of the cooperative RNAs. Cooperative binding between RNA and ATP substrates has been observed for the DEAD/H proteins eIF4A and Ded1p (*7*, *32*). With Ded1p, this cooperative binding was observed only with a duplex RNA molecule containing a ssRNA tail, suggesting the cooperativity in this system may depend on the presence of ssRNA or a ssRNA−dsRNA junction. This observation is consistent with the RNA requirements we see with DbpA.

This requirement for helix 89 and the correlation to activity in other systems may imply that helix 89 is the preferred target of DbpA's helicase activity in the R153 substrate. In the context of the ribosome, mutations of nucleotides within helix 89 (U2460, G2490, U2492, and U2493) affect translational accuracy and could emphasize the importance of proper folding of this region (*54*). Pseudouridines at U2457, U2504, U2580, or U2605 (*55*) could also require DbpA's helicase activity for efficient processing. Modulation of RNA structure by DbpA may also be required for proper organization of the central loop region of domain V and in establishing proper interactions with nearby ribosomal proteins, which include L2, L3, L6, L10, and L14 (*56*, *57*).

In vitro helicase assays have demonstrated unwinding in the context of a bimolecular version of the R32 substrate (*17*). Our binding studies would indicate that such small helicase substrates lack the RNA elements required for cooperative binding with ATP which result in less efficient energetic coupling between ATP hydrolysis and helicase activity. Indeed, while an ATP hydrolysis rate of 250 min^{-1} is observed, helicase rates of R32 are $\sim$0.1 min^{-1}. This discrepancy suggests the helicase substrates tested thus far have been sub-optimal and may be reconciled by helicase substrates that include helix 89. Further experiments with these bimolecular constructs are required to establish relationships between cooperative binding and coupled enzyme activities.

We can cast these results in the context of the structural model derived from the ATPase activity assays that described two sets of protein−RNA contacts, one with the C-terminal domain and one with the conserved DEAD motifs (*16*). Our results would suggest three sets of independent contacts to hairpin 92, helix 90, and helix 89. Since hairpin 92 and helix 90 are involved in high affinity and sequence-specific binding, we propose that these contacts come from the C-terminal domain of the DbpA protein which has been shown to confer specificity to this system (*12*, Kossen and Uhlenbeck, unpublished results). The cooperative contacts to helix 89 are most likely conferred through the active helicase site (the conserved DEAD motifs), since cooperativity responds to the ATP hydrolysis cycle.

An alternative model explaining the requirement for helix 89 in cooperative binding is that this helix may be a structural element required for organization of another target site within R153. Although the structure of R153 in solution is unknown, the structure of this region within the ribosome is quite compact (*58*). In that structure, helix 90 and helix 91 are coaxially stacked and packed against helix 89 and a long-range base pair occurs between C2475 and G2529. G2553 interacts with the C2507−G2582 base pair to form a long-range triple that co-localizes the identity elements within hairpin 92 and helix 90. It is possible that DbpA recognizes aspects of this structure in cooperative binding which are lost when helix 89 is removed. In this case, helicase substrates including helix 89 could enhance the unwinding of other target helices within R153 or perhaps in other regions of 23S rRNA.

ACKNOWLEDGMENT

The authors thank Michael O'Connor and Al Dahlberg for providing U2555 mutant expression plasmids. We also thank Camille Diges, Fedor Karginov, and Karl Kossen for many helpful discussions and critical reading of the manuscript.

REFERENCES

1. Linder, P., and Daugeron, M. C. (2000) *Nat. Struct. Biol. 7*, 97−99.
2. de la Cruz, J., Kressler, D., and Linder, P. (1999) *Trends Biochem. Sci. 24*, 192−198.
3. Herschlag, D. (1995) *J. Biol. Chem. 270*, 20871−20874.
4. Wassarman, D. A., and Steitz, J. A. (1991) *Nature 349*, 463−464.
5. Luking, A., Stahl, U., and Schmidt, U. (1998) *Crit. Rev. Biochem. Mol. Biol. 33*, 259−296.
6. Regnier, P., and Arraiano, C. M. (2000) *Bioessays 22*, 235−244.
7. Lorsch, J. R., and Herschlag, D. (1998) *Biochemistry 37*, 2180−2193.
8. Lorsch, J. R., and Herschlag, D. (1998) *Biochemistry 37*, 2194−2206.
9. Jankowsky, E., Gross, C. H., Shuman, S., and Pyle, A. M. (2000) *Nature 403*, 447−451.
10. Wong, I., and Lohman, T. M. (1996) *Proc. Natl. Acad. Sci. U.S.A. 93*, 10051−10056.
11. Lohman, T. M., and Bjornson, K. P. (1996) *Annu. Rev. Biochem. 65*, 169−214.
12. Kossen, K., and Uhlenbeck, O. C. (1999) *Nucleic Acids Res. 27*, 3811−3820.
13. Nicol, S. M., and Fuller-Pace, F. V. (1995) *Proc. Natl. Acad. Sci. U.S.A. 92*, 11681−11685.
14. Tsu, C. A., and Uhlenbeck, O. C. (1998) *Biochemistry 37*, 16989−16996.
15. Boddeker, N., Stade, K., and Franceschi, F. (1997) *Nucleic Acids Res. 25*, 537−545.
16. Tsu, C. A., Kossen, K., and Uhlenbeck, O. C. (2001) *RNA 7*, 702−709.
17. Diges, C. M., and Uhlenbeck, O. C. (2001) *EMBO J. 20*, 5503−5512.
18. Milligan, J. F., and Uhlenbeck, O. C. (1989) *Methods Enzymol. 180*, 51−62.
19. Dertinger, D., and Uhlenbeck, O. C. (2001) *RNA 7*, 622−631.
20. Witherell, G. W., Wu, H. N., and Uhlenbeck, O. C. (1990) *Biochemistry 29*, 11051−11057.
21. Pugh, G. E., Nicol, S. M., and Fuller-Pace, F. V. (1999) *J. Mol. Biol. 292*, 771−778.
22. Henn, A., Medalia, O., Shi, S. P., Steinberg, M., Franceschi, F., and Sagi, I. (2001) *Proc. Natl. Acad. Sci. U.S.A. 10*, 10.
23. Fried, M., and Crothers, D. M. (1981) *Nucleic Acids Res. 9*, 6505−6525.
24. Carey, J. (1988) *Proc. Natl. Acad. Sci. U.S.A. 85*, 975−979.
25. Lane, D., Prentki, P., and Chandler, M. (1992) *Microbiol. Rev. 56*, 509−528.
26. Cann, J. R., Pfenninger, O., and Pettijohn, D. E. (1995) *Electrophoresis 16*, 881−887.
27. Cann, J. R. (1996) *Electrophoresis 17*, 1535−1536.
28. Cann, J. R. (1998) *Electrophoresis 19*, 127−141.
29. Molloy, P. L. (2000) *Methods Mol. Biol. 130*, 235−246.
30. Uhlenbeck, O. C. (1972) *J. Mol. Biol. 65*, 25−41.
31. Gulick, A. M., Bauer, C. B., Thoden, J. B., and Rayment, I. (1997) *Biochemistry 36*, 11619−11628.
32. Iost, I., Dreyfus, M., and Linder, P. (1999) *J. Biol. Chem. 274*, 17677−17683.
33. Jezewska, M. J., and Bujalowski, W. (1996) *J. Biol. Chem. 271*, 4261−4265.
34. Hingorani, M. M., and Patel, S. S. (1996) *Biochemistry 35*, 2218−2228.
35. Hingorani, M. M., and Patel, S. S. (1993) *Biochemistry 32*, 12478−12487.
36. Wong, I., Chao, K. L., Bujalowski, W., and Lohman, T. M. (1992) *J. Biol. Chem. 267*, 7596−7610.
37. Brendza, K. M., Sontag, C. A., Saxton, W. M., and Gilbert, S. P. (2000) *J. Biol. Chem. 275*, 22187−22195.

38. Kozielski, F., Sack, S., Marx, A., Thormahlen, M., Schonbrunn, E., Biou, V., Thompson, A., Mandelkow, E. M., and Mandelkow, E. (1997) *Cell 91*, 985−994.
39. Furch, M., Fujita-Becker, S., Geeves, M. A., Holmes, K. C., and Manstein, D. J. (1999) *J. Mol. Biol. 290*, 797−809.
40. Rayment, I., Smith, C., and Yount, R. G. (1996) *Annu. Rev. Physiol. 58*, 671−702.
41. Smith, C. A., and Rayment, I. (1996) *Biophys. J. 70*, 1590−1602.
42. Pai, E. F., Krengel, U., Petsko, G. A., Goody, R. S., Kabsch, W., and Wittinghofer, A. (1990) *EMBO J. 9*, 2351−2359.
43. Schlichting, I., Almo, S. C., Rapp, G., Wilson, K., Petratos, K., Lentfer, A., Wittinghofer, A., Kabsch, W., Pai, E. F., Petsko, G. A. et al. (1990) *Nature 345*, 309−315.
44. Sprang, S. R. (1997) *Annu. Rev. Biochem. 66*, 639−678.
45. Waksman, G., Lanka, E., and Carazo, J. M. (2000) *Nat. Struct. Biol. 7*, 20−22.
46. West, S. C. (1996) *Cell 86*, 177−180.
47. Leibler, S., and Huse, D. A. (1993) *J. Cell Biol. 121*, 1357−1368.
48. Krupka, R. M. (1998) *Exp. Physiol. 83*, 243−251.
49. Krupka, R. M. (1996) *Biophys. J. 70*, 1863−1871.
50. Shuman, S. (1993) *J. Biol. Chem. 268*, 11798−11802.
51. Rozen, F., Edery, I., Meerovitch, K., Dever, T. E., Merrick, W. C., and Sonenberg, N. (1990) *Mol. Cell. Biol. 10*, 1134−1144.
52. Hirling, H., Scheffner, M., Restle, T., and Stahl, H. (1989) *Nature 339*, 562−624.
53. Lain, S., Riechmann, J. L., and Garcia, J. A. (1990) *Nucleic Acids Res. 18*, 7003−7006.
54. O'Connor, M., Brunelli, C. A., Firpo, M. A., Gregory, S. T., Lieberman, K. R., Lodmell, J. S., Moine, H., Van Ryk, D. I., and Dahlberg, A. E. (1995) *Biochem. Cell Biol. 73*, 859−868.
55. Bakin, A., and Ofengand, J. (1993) *Biochemistry 32*, 9754−9762.
56. Baranov, P. V., Sergiev, P. V., Dontsova, O. A., Bogdanov, A. A., and Brimacombe, R. (1998) *Nucleic Acids Res. 26*, 187−189.
57. Yusupov, M. M., Yusupova, G. Z., Baucom, A., Lieberman, K., Earnest, T. N., Cate, J. H., and Noller, H. F. (2001) *Science 292*, 883−896.
58. Ban, N., Nissen, P., Hansen, J., Moore, P. B., and Steitz, T. A. (2000) *Science 289*, 905−920.

BI012062N